JOURNAL OF GUIDANCE, CONTROL, AND DYNAMICS
Vol. 30, No. 1, January–February 2007

Terminal Guidance for an Unpowered Reusable Launch Vehicle with Bank Constraints

C. A. Kluever*
University of Missouri-Columbia, Columbia, Missouri 65211

DOI: 10.2514/1.24864

A new guidance scheme has been developed for the terminal phase of an unpowered reusable launch vehicle that has known limited bank capabilities. Reduced bank angle magnitude may be the result of actuator failures, and in such cases a vehicle will have difficulty performing the required heading change before approach and landing. A vertical guidance law controls dynamic pressure, and attempts to track the minimum dynamic pressure boundary to extend the ground track and maximize the turning rate. Lateral guidance uses a bank reversal to widen the turn radius and spiral in to a heading-alignment circle. The guidance algorithm iterates on two parameters (bank-reversal switch time and heading-alignment circle location), and selects the best values by propagating several trajectories to the desired approach and landing energy state. The effectiveness of the guidance algorithm is demonstrated by several numerical simulations, which show that the guided vehicle is able to successfully reach the desired approach and landing interface state with bank limitations as low as 18 deg.

Nomenclature

C_D = drag coefficient
C_{D0} = zero-lift drag coefficient
C_L = lift coefficient
D = drag force, lb
E = energy height, ft
G_H = altitude error gain, ft^{-1}
G_{HD} = altitude-rate error gain, s/ft
G_Q = dynamic pressure error gain, ft^2/lb
G_{QD} = dynamic pressure rate gain, $\text{s} \cdot \text{ft}^2/\text{lb}$
G_R = HAC radius error gain, rad/ft
G_{RD} = HAC radius rate gain, $\text{rad} \cdot \text{s/ft}$
G_Y = cross-track gain, rad/ft
G_{YD} = cross-track rate gain, $\text{rad} \cdot \text{s/ft}$
G_ϕ = heading error gain, rad/rad
g = Earth's gravitational acceleration, 32.174 ft/s^2
h = altitude above runway, ft
J = normalized terminal state error
K = lift-induced drag coefficient parameter
L = lift force, lb
m = vehicle mass, slugs
N = drag polar exponent
n_Z = vehicle acceleration along negative z-body axis, g
$\bar{q}$ = dynamic pressure, lb/ft^2
R = instantaneous turn radius, ft
R_F = heading-alignment circle (or cone) radius, ft
R_2 = quadratic coefficient for heading-alignment cone radius, ft/rad^2
S = vehicle reference area, ft^2
s = ground-track range, ft
t = time, s
t_ϕ = switch time for bank reversal, s
V = airspeed, ft/s
x = downtrack position along runway centerline, ft
y = cross-track position with respect to runway centerline, ft
α = angle of attack, rad
β = inverse scale height, ft^{-1}
γ = flight-path angle, rad
ϕ = bank angle, rad
ρ = atmospheric density, slugs/ft^3
ψ = heading angle, rad

Subscripts

ALI = approach and landing interface
f = final value
go = range-to-go value
HAC = heading-alignment cone (or circle)
ref = reference value
SL = sea-level value
0 = initial value

Introduction

A major objective of a next-generation reusable launch vehicle (RLV) includes significant improvements in vehicle safety, reliability, and operation costs. A specific goal is to reduce the probability of a catastrophic failure from 1 in 500 missions (the current space shuttle goal) to 1 in 10,000 missions [1]. Hanson [1,2] has argued that advanced guidance and control (AG&C) technologies will greatly improve the overall safety and reliability of future RLV missions. In particular, AG&C methods may be able to safely return an RLV that is plagued by scenarios such as vehicle mismodeling that results in control problems, aerosurface failures, poor vehicle performance, and larger than expected flight dispersions. Advanced guidance methods have been developed for the ascent and entry phases of an RLV [3–9], whereas advanced control methods have been developed for attitude control and control allocation [10–13].

Terminal area energy management (TAEM) is a critical flight phase that brings an unpowered RLV from the end of the entry phase to the approach and landing interface (ALI) point. For the U.S. Space Shuttle, TAEM begins at approximately Mach 2 and ALI is nominally at 10,000 ft altitude and Mach 0.5. TAEM guidance must take a vehicle from an arbitrary runway-relative heading and align it with the runway for proper approach and landing (A&L), and the space shuttle TAEM guidance does this by flying the vehicle to and around a heading-alignment cone (HAC), followed by a straightline path to ALI aligned with the runway centerline [14–16]. Although the shuttle's TAEM guidance has proven to be effective, it nevertheless relies on a small number of fixed, predetermined

Received 28 April 2006; revision received 9 June 2006; accepted for publication 13 June 2006.

*Professor, Mechanical and Aerospace Engineering Department. Associate Fellow AIAA

reference trajectories. For example, the shuttle's TAEM guidance can select two discrete HAC positions (a nominal and a minimum-energy HAC location), and two discrete reference altitude profiles that depend on vehicle weight.

Onboard trajectory generation may offer a potentially advantageous AG&C technique that can safely and reliably deliver an RLV to the proper ALI state in the presence of extreme conditions. Recently, researchers have investigated onboard trajectory planning for the A&L phase of an RLV. Schierman et al. [17] have developed a trajectory reshaping algorithm which interrogates a neural network that stores a database of precomputed optimal A&L trajectories that span the expected values for the vehicle states and critical parameters (such as vehicle drag). Barton and Tragesser [18] present an automated trajectory design algorithm for the A&L phase of the X-34, and their algorithm computes the angle and location of a steep glide slope for flight at constant dynamic pressure. Kluever [19] developed a trajectory-planning algorithm that computes a feasible A&L path by iterating on a single geometric parameter (flight-path angle for the final flare).

Despite the recent abundant work in applying AG&C concepts to the A&L problem, it appears that fewer researchers have focused on advanced TAEM guidance designs. Burchett [20] developed a TAEM guidance method based on fuzzy logic which is capable of handling trajectory constraints. Grantham [21] presents a guidance method based on an adaptive critic neural network, and this work presents trajectories with limited heading changes. Da Costa [22] developed a TAEM trajectory-planning algorithm for an RLV that relies on onboard trajectory optimization techniques using nonlinear programming concepts to obtain feasible paths. Hull et al. [23] developed a guidance technique for both the TAEM and A&L phases of an RLV. Their proposed onboard guidance approach modeled the reference path with a small number of trajectory parameters, and then reshaped the reference trajectory to compensate for changes in vehicle aerodynamics due to aerosurface failures. Kluever and Horneman [24] present a shuttle-based TAEM guidance method that recomputes a new reference trajectory by iterating on geometric parameters.

This paper presents a TAEM guidance method for a scenario where the banking capabilities of the RLV are compromised, perhaps due to aerosurface failures. When significant bank constraints exist, an RLV will be unable to use a shuttle-based guidance method where the vehicle attempts to follow a preplanned altitude reference profile and HAC ground-track for heading alignment. The proposed TAEM guidance algorithm computes the best feasible path from the current state to the desired ALI state by numerically propagating several trajectories (with known bank angle magnitude limits) and iterating on two guidance parameters. Once the best feasible path is identified, it is used as a reference for closed-loop TAEM guidance. Although the proposed TAEM guidance method shares similar concepts with the shuttle approach, the structure of the reference path is significantly different. The effectiveness of the proposed guidance algorithm is demonstrated by numerically simulating TAEM scenarios for a range of bank angle limitations.

System Models

Equations of Motion

The unpowered RLV is considered as a point mass, and its three-dimensional gliding motion is defined by

$$\dot{V} = \frac{-D}{m} - g\sin\gamma \tag{1}$$

$$\dot{\gamma} = \frac{L\cos\phi}{mV} - \frac{g}{V}\cos\gamma \tag{2}$$

$$\dot{\psi} = \frac{L\sin\phi}{mV\cos\gamma} \tag{3}$$

$$\dot{h} = V\sin\gamma \tag{4}$$

$$\dot{x} = V\cos\gamma\cos\psi \tag{5}$$

$$\dot{y} = V\cos\gamma\sin\psi \tag{6}$$

where lift and drag forces are defined in the usual manner:

$$L = \bar{q}SC_L \tag{7}$$

$$D = \bar{q}SC_D \tag{8}$$

and dynamic pressure is $\bar{q} = \rho V^2/2$. The governing equations of motion (1–6) are with respect to a "flat-Earth" model, where the $+x$-axis points along the runway centerline on approach, the $+y$-axis points right of the runway on approach, the $+z$-axis points below the surface, and the origin is at the runway threshold. Flight-path angle is measured from the xy (horizontal) plane to the velocity vector. Vehicle heading is measured clockwise from the runway centerline on approach. Atmospheric density is computed using the standard atmosphere.

Vehicle Models

The X-33 is the test vehicle for guidance algorithm development. This vehicle was used because much of the previous work in the AG&C program (such as entry and ascent guidance) used the X-33, and therefore the vehicle parameters and aerodynamic characteristics were readily available. A standard drag polar is used to model the X-33 aerodynamics:

$$C_D = C_{D0} + KC_L^N \tag{9}$$

Zero-lift drag coefficient C_{D0}, lift-induced drag coefficient parameter K, and exponent N are obtained by fitting the drag polar (9) to the "true" aerodynamic data from two-dimensional lookup tables that are functions of Mach number and angle of attack. The guidance method requires a simple aerodynamic model of the X-33 to propagate trajectories. Table 1 presents discrete values of the drag polar parameters at six discrete Mach numbers that span the TAEM flight regime. The guidance algorithm estimates the drag coefficient by using Eq. (9) with a known value of C_L, and interpolated values of K, C_{D0}, and N, which are computed by linear interpolation among the data in Table 1 with Mach number as the independent variable.

Shuttle TAEM Guidance

Before discussing the new TAEM guidance for bank constraints, it is instructive to briefly review the space shuttle's TAEM guidance. The shuttle TAEM guidance relies on a small set of preplanned reference profiles for altitude and energy height vs ground-track range to the runway. Predicted ground-track range is estimated by piecing together three flight phases: acquisition, heading alignment, and prefinal. Figure 1 shows these three guidance phases. During the acquisition phase, the ground track is estimated by assuming a constant-radius turn to a straightline path that is tangent to the heading-alignment cone. Ground track during the HAC turn is

Table 1 Drag polar parameters for the X-33

Mach	C_{D0}	K	N
0.5	0.0970	0.2123	2.3
1.0	0.2343	0.3501	2.4
1.5	0.2348	0.4377	2.1
2.0	0.2040	0.5624	2.0
2.5	0.1828	0.6782	2.0
3.0	0.1695	0.7165	1.9

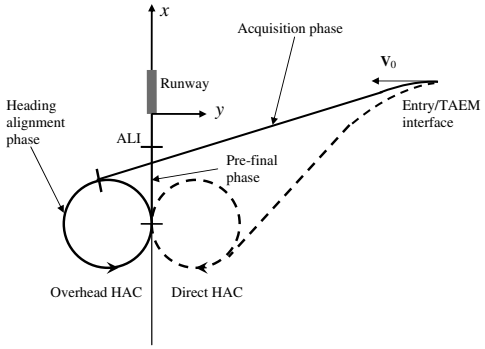

Fig. 1 Shuttle TAEM guidance phases (solid line: overhead HAC; dashed line: direct HAC).

computed from the turn radius, which is a quadratic function of the HAC turn angle ($\Delta\psi_{\text{HAC}}$):

$$R_{\text{HAC}} = R_F + R_2\Delta\psi_{\text{HAC}}^2 \tag{10}$$

where R_F is the final HAC radius and R_2 is a constant coefficient. Integrating Eq. (10) with respect to turn angle yields the ground-track range of the HAC turn:

$$s_{\text{HAC}} = R_F\Delta\psi_{\text{HAC}} + \frac{1}{3}R_2\Delta\psi_{\text{HAC}}^3 \tag{11}$$

Figure 1 presents both the so-called overhead and direct HAC configurations. An overhead HAC (solid line in Fig. 1) is on the opposite side of the runway as the approaching RLV, and the ensuing turn angle is greater than 180 deg. A direct HAC is located on the same side of the runway as the approaching RLV, and the corresponding HAC turn angle is less than 180 deg (dashed line in Fig. 1). Finally, the prefinal ground-track range is simply the straightline segment distance from the x-axis location of the HAC center to the ALI point.

The shuttle TAEM guidance attempts to track a reference altitude profile that is a cubic function of predicted ground-track range to ALI. An open-loop, equilibrium glide normal acceleration command is augmented by closed-loop commands based on altitude and altitude-rate errors. The n_Z command is limited and filtered by comparing the vehicle's current energy and dynamic pressure to preplanned reference profiles that are also functions of predicted ground track to ALI. Lateral guidance commands for the acquisition phase are proportional to heading error. Bank command for the heading-alignment phase consists of an open-loop term based on the HAC radius plus feedback terms proportional to radius and radius-rate errors. Bank command for cross-range control of the prefinal phase is simply proportional to the lateral runway offset distance (y) and its time-rate of change. Details of the shuttle TAEM guidance can be found in [14–16].

TAEM Guidance with Bank Limits

Motivation and Assumptions

In [24], a new TAEM guidance algorithm was developed using the basic structure of the shuttle TAEM guidance described in the preceding section. In this new approach, three fundamental geometric parameters (downtrack HAC location x_{HAC}, final HAC radius R_F, and quadratic HAC coefficient R_2) are varied and the onboard guidance scheme propagates multiple trajectories to ALI. Infeasible trajectories that violate control and operational constraints (such as maximum dynamic pressure) are discarded, and the best feasible trajectory is selected as the reference path for the shuttle-based closed-loop guidance method. This method is applied to TAEM scenarios with dispersions in initial heading, initial altitude (energy), and drag coefficient, and the results presented in [24] show that the shuttle-based guidance coupled with onboard trajectory-planning demonstrates significant improvements when compared to guidance with a single fixed reference trajectory. However, whereas the methods of [24] expand the envelope of feasible TAEM trajectories, the method nevertheless produces neighboring paths that show the same basic characteristics of a nominal TAEM trajectory.

It is highly unlikely that the neighboring-path guidance method will successfully control an RLV with severe operational limitations. For example, if banking capabilities are limited, it is unlikely that a crippled RLV could successfully complete the TAEM trajectory by flying directly to the HAC tangency point and tracking the HAC with a banked turn (typically, bank angle ranges from 45 to 55 deg during a nominal HAC turn). In this scenario, both the vertical and lateral guidance channels must be altered because a neighboring-path method will not be successful.

In [24], Kluever and Horneman obtained optimal TAEM trajectories using an inverse-dynamics approach and nonlinear programming methods. An optimal path was found for the case with 20-deg limits on bank angle, and the optimal bank profile showed a "bang-bang" structure where the RLV initially applied full bank ($\phi = +20$ deg) away from a nominal HAC location to increase ground-track distance, and then switched to $\phi = -20$ deg to "spiral in" to the proper runway heading. Consequently, the total ground track distance was nearly 30% greater than a nominal ground track. The optimal vertical flight path also showed two significant pull-up maneuvers that served to modulate dynamic pressure and extend ground range. Clearly, shuttle TAEM guidance and a neighboring reference path are not able to successfully guide an RLV with bank limitations.

Before the guidance laws are presented in detail, the main assumptions behind the proposed method are discussed. First, it is assumed that guidance has knowledge of the magnitude of any bank limitations. This information could possibly be derived from in-flight monitoring of aerosurface actuators. Second, it is assumed that guidance has knowledge of vehicle aerodynamics and atmospheric conditions. Initially, the guidance method would use the simplified drag polar model previously described (with curve-fit parameters over the expected Mach range) as a nominal aerodynamic database. Accelerometer measurements could be used to estimate bias terms for lift and drag coefficients, which in turn could augment and improve the accuracy of the nominal drag polar model. This approach has been proposed by Hull et al. [23] for onboard estimation of the aerodynamic coefficients required by a guidance scheme. Finally, the nominal atmospheric model could be updated by incorporating the available onboard air data system and navigation information.

Vertical Guidance Laws

The proposed TAEM guidance method for a bank-limited RLV is developed by judicious selection of both vertical and lateral guidance laws. To begin the analysis, first observe turn radius:

$$R = \frac{V^2\cos\gamma}{g\tan\phi} \tag{12}$$

Obviously, a small bank angle ϕ will increase the turn radius. To reduce the turn radius, Eq. (12) shows that it is desirable to perform the turn with the lowest possible airspeed. Airspeed can be minimized at altitude by flying the RLV at the lowest acceptable dynamic pressure. For the X-33, the minimum dynamic pressure boundary is 80 lb/ft^2. Minimum dynamic pressure can be achieved by flying the RLV at a relatively shallow flight-path angle, which will tend to extend the overall range of the RLV. Extending the total range is desirable, because a bank-limited RLV must first widen the turn radius and then "spiral in" toward the runway centerline; a crippled RLV cannot simply fly directly to a HAC tangency point and perform a relatively tight HAC turn. Therefore, our vertical guidance law will employ a dynamic pressure tracking scheme, rather than an altitude-tracking scheme like shuttle TAEM guidance. The guidance command for lift coefficient is

$$C_L = C_L^* + G_Q(\bar{q}_{\text{ref}} - \bar{q}) + G_{QD}\dot{\bar{q}} \tag{13}$$

where C_L^* is an open-loop reference lift coefficient required to maintain a constant flight-path angle ("quasi-equilibrium glide"):

$$C_L^* = \frac{mg\cos\gamma}{\bar{q}S\cos\phi} \tag{14}$$

Reference lift coefficient can be computed by setting the dynamical flight-path Eq. (2) to zero. Note that the bank angle ϕ must first be determined by the lateral guidance law (to be discussed). Equation (13) is a proportional-derivative control law for lift, and the time-rate of dynamic pressure is

$$\dot{\bar{q}} = \frac{1}{2}\frac{\mathrm{d}\rho}{\mathrm{d}h}\frac{\mathrm{d}h}{\mathrm{d}t}V^2 + \rho V\frac{\mathrm{d}V}{\mathrm{d}t} \tag{15}$$

After substituting the kinematic relation (4) for $\mathrm{d}h/\mathrm{d}t$ and the dynamical Eq. (1) for $\mathrm{d}V/\mathrm{d}t$, we obtain

$$\dot{\bar{q}} = V\sin\gamma\left[\left(\frac{\rho'}{\rho} - \frac{\rho SC_D}{m\sin\gamma}\right)\bar{q} - \rho g\right] \tag{16}$$

where $\rho' = \mathrm{d}\rho/\mathrm{d}h$, which is computed from an exponential atmospheric density model

$$\frac{\mathrm{d}\rho}{\mathrm{d}h} = -\beta\rho_{SL}\exp(-\beta h) \tag{17}$$

where the inverse scale height is $\beta = 1/30,499\ \mathrm{ft}^{-1}$. Therefore, the ratio ρ'/ρ in Eq. (16) is equal to $-\beta$.

Vertical guidance law (13) is used to track the minimum dynamic pressure boundary to allow significant changes in heading. It is worth noting that unlike shuttle guidance, the proposed vertical guidance method does not rely on a predetermined ground-track pattern and ground-track range-to-go prediction.

When the RLV has nearly acquired the proper heading relative to the runway (for example, $|\psi| \leq 5$ deg), guidance switches to the prefinal phase and the vertical guidance law is based on an altitude reference profile h_{ref}:

$$C_L = C_L^* + G_H(h_{\mathrm{ref}} - h) + G_{HD}(\dot{h}_{\mathrm{ref}} - \dot{h}) \tag{18}$$

The reference steep glide slope has constant flight-path angle γ_{ALI}:

$$h_{\mathrm{ref}} = h_{\mathrm{ALI}} - s_{\mathrm{go}}\tan\gamma_{\mathrm{ALI}} \tag{19}$$

where s_{go} is the downtrack distance from the RLV to ALI, and is easily predicted based on knowledge of the vehicle's current downtrack position (x). The reference altitude-rate is

$$\dot{h}_{\mathrm{ref}} = V\sin\gamma_{\mathrm{ALI}} \tag{20}$$

Reference steep glide slope angle for A&L is $\gamma_{\mathrm{ALI}} = -25.2$ deg, ALI altitude (by definition) is $h_{\mathrm{ALI}} = 10,000$ ft, and downtrack location of ALI is fixed at $x_{\mathrm{ALI}} = -26,316$ ft (see [19]). The target equivalent airspeed for ALI is 457 ft/s (or, $V = 570$ ft/s at ALI altitude), which produces a quasi-equilibrium glide for A&L with nearly constant $\bar{q} = 248\ \mathrm{lb/ft}^2$. Because the RLV will be flying at a relatively shallow flight-path angle as it tracks the lower boundary for dynamic pressure, Eq. (18) will initially cause the vehicle to dive and acquire the A&L steep glide slope when guidance switches to the prefinal phase. The dive is necessary to convert potential energy into kinetic energy and increase dynamic pressure to the desired value for A&L.

Lateral Guidance Laws

The proposed lateral guidance law for an RLV with bank limitation uses the "bang-bang" banking structure that appears in the optimal TAEM trajectories. Because our goal is to fly at minimum dynamic pressure and extend the ground track, the initial lateral command is the maximum allowable bank angle away from the HAC (this maneuver is similar to the so-called S-turn performed by the shuttle when it has excess energy). A full bank reversal is then commanded at switch time t_ϕ and the RLV begins to "spiral in" toward the HAC until it acquires a straightline heading to a HAC tangency point. Consequently, the HAC turn is relatively short, and the majority of the heading change is performed after the bank reversal before the RLV actually reaches the HAC. Once the RLV is on the HAC, the remainder of the lateral guidance is similar to the shuttle's guidance laws for the heading-alignment and prefinal phases.

After the RLV has performed the bank reversal and the remaining heading error is less than 180 deg, lateral guidance attempts to acquire the circular HAC. Bank angle command for the HAC acquisition phase is simply proportional to the heading error:

$$\phi = G_\phi\Delta\psi_{\mathrm{AT}} \tag{21}$$

where $\Delta\psi_{\mathrm{AT}}$ is the difference between the current heading and a heading tangent to the HAC.

Bank angle command for the HAC turn consists of open- and closed-loop terms:

$$\phi = \tan^{-1}\left(\frac{V^2\cos\gamma}{gR_F}\right) + G_R\Delta R + G_{RD}\dot{R} \tag{22}$$

where ΔR is the difference between the distance to the HAC center and the HAC radius. For the sake of simplicity, the HAC is a heading-alignment *cylinder* with constant radius R_F. Feedback terms proportional to radial error and radial rate augment an open-loop term that is the bank angle required to follow the circular HAC turn. HAC radius R_F is computed using Eq. (12) with the maximum available bank angle, airspeed V corresponding to the reference dynamic pressure (85 $\mathrm{lb/ft}^2$) at an altitude of 35,000 ft, and a nominal flight-path angle $\gamma = -14$ deg. These selected values represent an average altitude when the RLV initially reaches the HAC, and the approximate flight-path angle required to hold dynamic pressure constant at 85 $\mathrm{lb/ft}^2$. Therefore, using these values, the bank-limited RLV would be able to track a circular HAC at altitudes below 35,000 ft as airspeed decreases.

Guidance transitions to the prefinal phase when the heading error with respect to the runway becomes less than 5 deg. The commanded bank angle is simply proportional to cross-track error and cross-track rate:

$$\phi = -G_Y y - G_{YD}\dot{y} \tag{23}$$

In all cases, the bank angle command computed by Eqs. (21–23) is limited by the maximum bank capabilities of the crippled RLV.

Trajectory-Propagation Algorithm

The proposed TAEM guidance algorithm consists of the control laws for lift coefficient [Eqs. (13) or (18)] and bank angle [Eqs. (21–23)]. Table 2 summarizes the required guidance parameters, and shows which parameters are either fixed or determined by onboard calculations. Feedback gains are selected using numerical trials (some values are similar to shuttle gains), and the reference dynamic pressure $\bar{q}_{\mathrm{ref}}$ is set at 85 $\mathrm{lb/ft}^2$ because some undershoot is expected during the transient response. Two guidance parameters, bank-reversal switch time t_ϕ and downtrack HAC location x_{HAC}, are computed by iteration and onboard trajectory propagation.

The guidance algorithm propagates multiple TAEM trajectories from the RLV's current position to ALI to determine the best values for switch time t_ϕ and x_{HAC}. Trajectory propagation is performed by onboard numerical integration of the equations of motion with energy as the independent variable. Energy height is total mechanical energy divided by weight:

$$E = \frac{V^2}{2g} + h \tag{24}$$

The time derivative of energy height is

$$\dot{E} = \frac{V\dot{V}}{g} + \dot{h} \tag{25}$$

Table 2 TAEM guidance parameters

Guidance parameter	Description	Value
x_{HAC}	Downtrack HAC location	Determined by propagation and iteration
t_ϕ	Bank-reversal switch time	Determined by propagation and iteration
R_F	HAC radius	Determined by Eq. (12)
$\bar{q}_{\mathrm{ref}}$	Reference dynamic pressure	85 lb/ft^2
G_Q	Dynamic pressure error gain	-0.0025 ft^2/lb
G_{QD}	Dynamic pressure rate gain	0.08 s $\cdot$ ft^2/lb
G_H	Altitude error gain	0.0006 ft^{-1}
G_{HD}	Altitude-rate error gain	0.006 s/ft
G_ϕ	Heading error gain	3.5 rad/rad
G_R	HAC radius error gain	$8.727(10^{-5})$ rad/ft
G_{RD}	HAC radius-rate gain	$3.491(10^{-3})$ rad $\cdot$ s/ft
G_Y	Cross-track gain	$5.236(10^{-4})$ rad/ft
G_{YD}	Cross-track rate gain	$6.109(10^{-3})$ rad $\cdot$ s/ft

Substituting Eqs. (1) and (4) into Eq. (25) yields

$$\dot{E} = \frac{-DV}{mg} \tag{26}$$

Obviously, E is monotonically decreasing for an unpowered glider, and therefore it serves as a convenient independent variable for integration. Equations of motion (1–6) are divided by Eq. (26) to produce governing equations with respect to energy height, which can be integrated between known boundaries for E. From [19], the desired ALI state is airspeed $V_{\mathrm{ALI}} = 570$ ft/s, altitude $h_{\mathrm{ALI}} = 10,000$ ft, and therefore $E_{\mathrm{ALI}} = 15,049$ ft.

Trajectory propagation is performed by using a variable-step, second/third-order numerical integration routine. The goal is to quickly propagate tens of trajectories with sufficient accuracy. Numerical trials showed that about 100 integration steps were needed to accurately simulate a single TAEM trajectory to A&L interface.

For the test cases shown here, we span a fixed range of nine values each for switch time t_ϕ and x_{HAC}. Therefore, 81 trajectories are propagated, and the "best" propagated trajectory is determined by evaluating the normalized terminal state error at ALI:

$$J = \left|\frac{h_f - h_{\mathrm{ALI}}}{h_{\mathrm{ALI}}}\right| + \left|\frac{\gamma_f - \gamma_{\mathrm{ALI}}}{\gamma_{\mathrm{ALI}}}\right| + \left|\frac{x_f - x_{\mathrm{ALI}}}{x_{\mathrm{ALI}}}\right| \tag{27}$$

Note that final velocity error is not included in the terminal error function, because the trajectory is propagated to the proper terminal energy and therefore a small altitude error will result in a small velocity error. Any trajectory where the magnitude of the final heading angle error is greater than 5 deg is excluded from consideration. The propagated trajectory with the smallest value of J is used to set the reference values for switch time t_ϕ and x_{HAC} in the closed-loop simulation. Minimization is performed by enumeration and simply sorting the feasible values of J. If no feasible paths exist among the 81 propagated trajectories (this will certainly be the case as bank magnitude limit approaches zero), then the algorithm could select the propagated trajectory with the smallest final heading error. Finally, note that the task of propagating a set of 81 trajectories is performed only once and at the initiation of TAEM; in practice, the propagation technique could be performed periodically during flight to adapt to potential failures.

The computational efficiency of this "brute force" approach could possibly be improved by using a shooting method, where corrections to the two guidance parameters are computed by using a numerically derived sensitivity matrix of first-order partial derivatives of the terminal error functions with respect to the guidance parameters. For example, Hull et al. [23] demonstrated an in-flight shooting method for updating a small number of guidance parameters.

It should be noted that the vertical guidance law attempts to achieve the maximum loft capability by flying near the minimum dynamic pressure boundary. Therefore, significant aerodynamic or atmospheric dispersions (such as winds) may degrade the vehicle's ground-track capability and prevent the RLV from reaching ALI with sufficient energy. One possible remedy would be to update aerodynamic and atmospheric models through in-flight measurements. Another possible remedy would be to bias energy at ALI so that the RLV has additional margin for unmodeled dispersions.

Numerical Results

The initial TAEM state is taken from the end state of a nominal entry trajectory, with $h_0 = 91,628$ ft, $V_0 = 2999.3$ ft/s (Mach 3.03), $\gamma_0 = -6.66$ deg, $\psi_0 = 278.55$ deg, $x_0 = -17,208$ ft, and $y_0 = 177,451$ ft. The nominal ALI state is $h_{\mathrm{ALI}} = 10,000$ ft (by definition), $V_{\mathrm{ALI}} = 570$ ft/s (Mach 0.54), $\gamma_{\mathrm{ALI}} = -25.2$ deg, and $x_{\mathrm{ALI}} = -26,316$ ft, respectively. Michaels Army Air Field is the landing site (altitude above sea level is 4340 ft), and therefore the initial dynamic pressure is 176.5 lb/ft^2. As previously mentioned, the trajectory-propagation algorithm uses a second/third-order integration scheme to quickly numerically integrate 81 TAEM trajectories to determine the best values for switch time t_ϕ and x_{HAC}. Once these values are determined, the guided TAEM trajectory is simulated by numerically integrating the governing Eqs. (1–6) with a variable-step, fourth/fifth-order Runge–Kutta (RK) method. The desired time span for the numerical integration is divided into "guidance cycle" segments, and the variable-step, variable-order RK method is used to numerically integrate the governing equations over each guidance cycle. Vertical and lateral guidance commands (C_L and ϕ) are computed at the beginning of each guidance cycle and then held constant until the next guidance cycle. The fixed guidance cycle is set to 0.5 s. The final states of the RLV at ALI are determined by interpolating among the simulation data at the point where altitude is 10,000 ft (the transitional trigger between TAEM and A&L).

Table 3 presents the results of several guided TAEM trajectories for a range of bank limitations. HAC radius increases as the maximum bank angle decreases (as expected), and the HAC location generally moves closer to the runway as maximum bank angle decreases. The bank-reversal switch time t_ϕ remains in the 20–35 s range for all solutions. Table 3 shows that all guided TAEM solutions exhibit a good match between the final RLV states and the desired ALI states, although state errors at ALI increase as bank angle becomes more limited. The propagation algorithm was able to obtain a feasible TAEM trajectory for a bank limit as low as 18 deg, but the resulting trajectory is low on energy (airspeed) when the RLV reaches 10,000 ft and the transition to A&L. It is likely that the A&L trajectory-planning method presented in [19] would be able to reshape the A&L flight path to accommodate the low-energy state. For extremely low bank capabilities, it may be beneficial to move the target ALI downtrack position x_{ALI} closer to the runway to better accommodate low-energy conditions.

Figure 2a presents two TAEM ground tracks for the cases where bank angle magnitude limitations are 30 and 20 deg. The initial banked turn away from the HAC (positive bank) is apparent in both cases, and the two ground tracks show the subsequent inward spiral after the bank reversal. The RLV with 30-deg bank limits finally acquires the HAC when the remaining heading-to-go is about 168 deg. HAC acquisition is delayed for the 20-deg bank limit case

Table 3 TAEM solutions and RLV state at ALI for range of bank limitations[a]

Bank limits, deg	R_F, ft	x_{HAC}, ft	t_ϕ, s	V_f, ft/s	γ_f, deg	ψ_f, deg	x_f, ft	y_f, ft
30	14,704	−51, 316	35	577.0	−25.3	0.03	−26, 303	−2.2
25	18,205	−56, 316	20	576.2	−25.2	0.02	−26, 311	−0.8
20	23,324	−38, 191	25	548.0	−25.9	−0.27	−26, 213	7.8
18	26,127	−30, 941	25	465.8	−26.3	0.20	−26, 184	38.2

[a]Nominal ALI target: $V_{\mathrm{ALI}} = 570$ ft/s, $\gamma_{\mathrm{ALI}} = -25.2$ deg, $\psi_{\mathrm{ALI}} = 0$ deg, $x_{\mathrm{ALI}} = -26,316$ ft, $y_{\mathrm{ALI}} = 0$ ft.

because the RLV must make a wider turn, and the RLV acquires the HAC when the heading-to-go is about 62 deg. Both ground tracks are distinctly different from a nominal shuttle TAEM ground track, where the vehicle immediately acquires a spiral HAC and flies a straightline path to the tangency point.

Figure 2b presents the TAEM ground track using the shuttle-based guidance from [24] for the case where bank angle magnitude is limited to 20 deg. The RLV reaches the HAC tangency point, but drastically overshoots it and falls below the desired ALI energy level before the RLV can complete the heading alignment. Figure 2b clearly shows that an RLV with bank limitations cannot successfully reach ALI by using a nonadaptive, shuttle-based guidance method.

Figures 3–6 present time histories of several important states and controls for the 20-deg bank limit case. Figure 3 presents the bank profile, showing the bank reversal at 25 s and the brief straightline path to the HAC tangency point. Proper computation of the HAC radius is apparent, because the bank command does not saturate during the brief HAC turn. Bank command is discontinuous as the lateral guidance laws transition from the HAC phase [Eq. (22)] to the prefinal phase [Eq. (23)].

Profiles for dynamic pressure and flight-path angle are presented in Figs. 4 and 5, respectively. The effects of the $\bar{q}$-tracking guidance law are easily observed in both figures: dynamic pressure steadily decreases and tracks the 85 lb/ft^2 reference with relatively low transient overshoot (Fig. 4), and the flight-path angle initially increases to reduce $\bar{q}$ (Fig. 5). Flight-path angle eventually reaches a relatively shallow quasi-equilibrium glide at $\gamma = -13.7$ deg as a consequence of $\bar{q}$ tracking the 85 lb/ft^2 reference. Figures 4 and 5 also show the beginning of the prefinal phase (end of HAC turn), where the vertical guidance law transitions from a $\bar{q}$ reference to the steep glide slope reference ($\gamma_{\mathrm{ALI}} = -25.2$ deg) and the RLV dives to increase dynamic pressure for A&L. The final value of $\bar{q}$ at A&L interface is 230 lb/ft^2, which is close to the target value of 248 lb/ft^2.

Figure 6 shows the profile for normal acceleration along the negative z-body axis, or n_Z. Normal acceleration is related to the lift and drag accelerations:

$$n_Z = \frac{(L\cos\alpha + D\sin\alpha)}{mg} \tag{28}$$

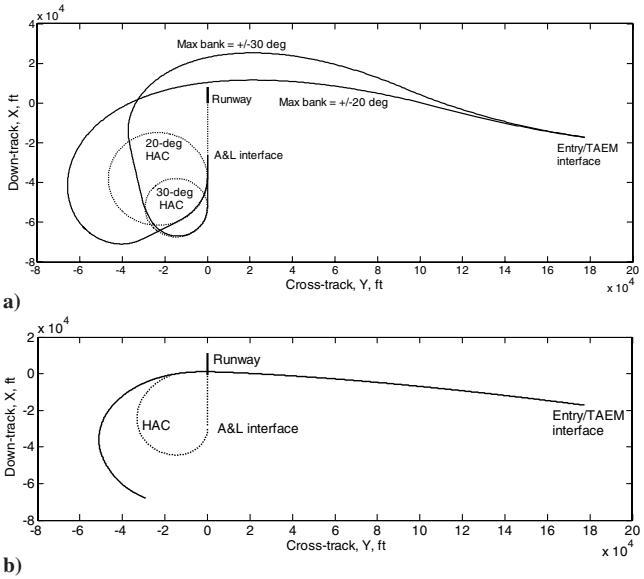

Fig. 2 TAEM ground tracks: a) 30-deg and 20-deg bank limits; b) shuttle-based guidance with 20-deg bank limits.

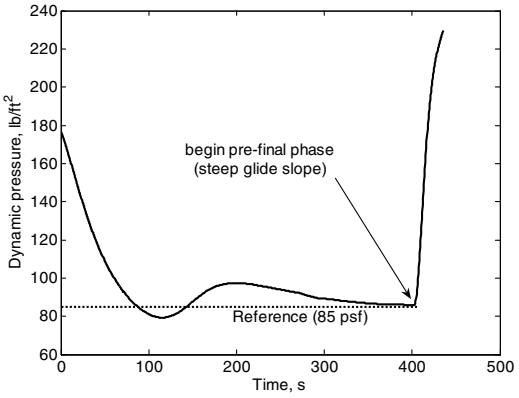

Fig. 4 Dynamic pressure profile for TAEM case with 20-deg bank limits.

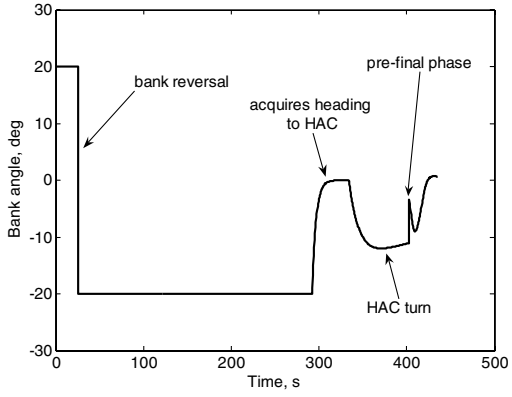

Fig. 3 Bank angle profile for TAEM case with 20-deg bank limits.

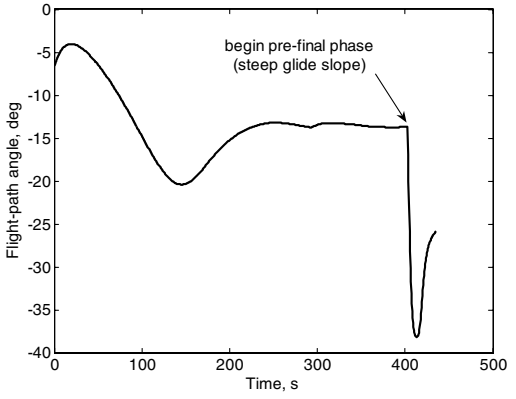

Fig. 5 Flight-path angle profile for TAEM case with 20-deg bank limits.

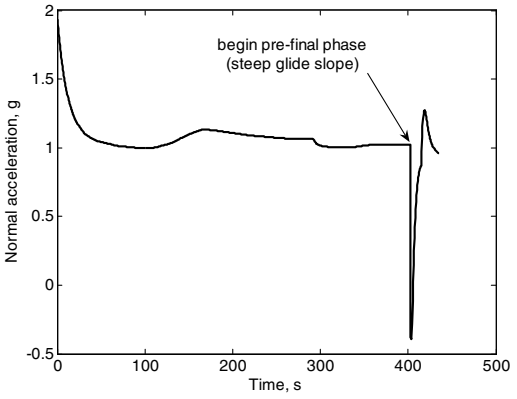

Fig. 6 Normal acceleration profile for TAEM case with 20-deg bank limits.

Here, lift and drag are computed from the vertical guidance command (C_L) and the drag polar, and angle of attack is estimated from a linear lift-slope profile. Although the vertical guidance formulation in this paper uses lift coefficient, a corresponding n_Z guidance command could be obtained from Eq. (28). Figure 6 shows the large initial n_Z command ($1.9g$) required for the pull-up maneuver to decrease flight-path angle and $\bar{q}$, followed by a relatively constant command for maintaining the reference dynamic pressure. At $t = 404$ s, the prefinal phase begins and the subsequent n_Z command is negative so that the RLV dives to acquire the steep glide slope. The subsequent angle-of-attack profile looks very similar to the n_Z profile shown in Fig. 6, with a maximum initial value of 20 deg (pull-up), steady-state value of about 12 deg ($\bar{q} = 85$ lb/ft^2 phase), minimum value of -4 deg (initial dive to the steep glide slope), and final value of 4 deg (ALI). This angle-of-attack history is within the acceptable limits of the X-33.

Conclusions

A new guidance scheme has been developed for the terminal flight phase of an unpowered reusable launch vehicle with bank magnitude limitations. It is highly unlikely that a crippled RLV with bank limitations will be able to successfully use a neighboring-path guidance method, such as the space shuttle's terminal area energy management guidance technique. The proposed guidance method maximizes the vehicle's limited turning ability by tracking the minimum dynamic pressure boundary and employing a bank-reversal scheme to widen the turn radius. Consequently, the resulting ground track and vertical profile of the terminal phase are significantly different from the shuttle's TAEM trajectory. The proposed guidance method employs an onboard trajectory-propagation algorithm that allows iteration on two guidance parameters (bank-reversal time and heading-alignment cylinder location) such that the proper vehicle state at approach and landing interface is achieved.

Several closed-loop simulations were conducted to demonstrate the proposed guidance algorithm. Scenarios involving a range of bank limitations were simulated, and the simulation results show that the new terminal guidance method was able to successfully deliver the RLV to the proper A&L state. The guided RLV successfully tracked the minimum dynamic pressure boundary, and this resulted in a relatively shallow flight-path angle and extended ground track range. The lateral guidance laws produce a wide inward spiral turn, followed by a relatively short circular turn for final heading alignment with the runway. Successful TAEM trajectories were obtained for bank limitations as low as 18 deg.

Based on these analyses, the proposed terminal guidance algorithm is a viable candidate for onboard implementation to improve the safety and reliability of future reusable launch vehicles. Further validation of this guidance method should include Monte Carlo simulations with dispersions in the initial state vector, vehicle aerodynamics, and atmospheric characteristics.

Acknowledgments

This research was supported by NASA Marshall Space Flight Center under the grant NAG8-1913. The author would like to thank John Hanson, Greg Dukeman, and Jack Mulqueen for their suggestions and help.

References

[1] Hanson, J. M., "A Plan for Advanced Guidance and Control Technology for 2nd Generation Reusable Launch Vehicles," AIAA Paper 02-4557, Aug. 2002.

[2] Hanson, J. M., "New Guidance for New Launch Vehicles," *Aerospace America*, Vol. 41, No. 3, March 2003, pp. 36–41.

[3] Dukeman, G. A., "Atmospheric Ascent Guidance for Rocket-Powered Launch Vehicles," AIAA Paper 02-4559, Aug. 2002.

[4] Lu, P., Sun, H., and Tsai, B., "Closed-Loop Endoatmospheric Ascent Guidance," *Journal of Guidance, Control, and Dynamics*, Vol. 26, No. 2, 2003, pp. 283–294.

[5] Calise, A., and Brandt, N., "Generation of Launch Vehicle Abort Trajectories Using a Hybrid Optimization Method," AIAA Paper 02-4560, Aug. 2002.

[6] Dukeman, G. A., "Profile-Following Entry Guidance Using Linear Quadratic Regulator Theory," AIAA Paper 02-4457, Aug. 2002.

[7] Zimmerman, C., Dukeman, G., and Hanson, J., "Automated Method to Compute Orbital Reentry Trajectories with Heating Constraints," *Journal of Guidance, Control, and Dynamics*, Vol. 26, No. 4, 2003, pp. 523–529.

[8] Shen, Z., and Lu, P., "Onboard Generation of Three-Dimensional Constrained Entry Trajectories," *Journal of Guidance, Control, and Dynamics*, Vol. 26, No. 1, 2003, pp. 111–121.

[9] Chen, D. T., Saraf, A., Leavitt, J. A., and Mease, K. D., "Performance of Evolved Acceleration Guidance Logic for Entry (EAGLE)," AIAA Paper 02-4456, Aug. 2002.

[10] Shtessel, Y., Zhu, J., and Daniels, D., "Reusable Launch Vehicle Attitude Control Using a Time-Varying Sliding Mode Control Technique," AIAA Paper 02-4779, Aug. 2002.

[11] Hodel, A. S., and Callahan, R., "Autonomous Reconfigurable Control Allocation (ARCA) for Reusable Launch Vehicles," AIAA Paper 02-4777, Aug. 2002.

[12] Doman, D. B., and Ngo, A. D., "Dynamic Inversion-Based Adaptive/Reconfigurable Control of the X-33 on Ascent," *Journal of Guidance, Control, and Dynamics*, Vol. 25, No. 2, 2002, pp. 275–284.

[13] Johnson, E. N., and Calise, A. J., "Limited Authority Adaptive Flight Control for Reusable Launch Vehicles," *Journal of Guidance, Control, and Dynamics*, Vol. 26, No. 6, 2003, pp. 906–913.

[14] Ehlers, H. L., and Kraemer, J. W., "Shuttle Orbiter Guidance System for the Terminal Flight Phase," *Automatica*, Vol. 13, No. 1, 1977, pp. 11–21.

[15] Anon., "MCC Level C Formulation Requirements: Shuttle TAEM Guidance and Control," NASA TM-80796, April 1980.

[16] Moore, T. E., "Space Shuttle Entry Terminal Area Energy Management," NASA TM-104744, Nov. 1991.

[17] Schierman, J. D., Hull, J. R., and Ward, D. G., "Adaptive Guidance with Trajectory Reshaping for Reusable Launch Vehicles," AIAA Paper 02-4458, Aug. 2002.

[18] Barton, G. H., and Tragesser, S. G., "Autolanding Trajectory Design for the X-34," AIAA Paper 99-4161, Aug. 1999.

[19] Kluever, C. A., "Unpowered Approach and Landing Guidance Using Trajectory Planning," *Journal of Guidance, Control, and Dynamics*, Vol. 27, No. 6, 2004, pp. 967–974.

[20] Burchett, B. T., "Fuzzy Logic Trajectory Design and Guidance for Terminal Area Energy Management," *Journal of Spacecraft and Rockets*, Vol. 41, No. 3, 2004, pp. 444–450.

[21] Grantham, K., "Adaptive Critic Neural Network Based Terminal Area Energy Management/Entry Guidance," AIAA Paper 2003-0305, Jan. 2003.

[22] Da Costa, R. R., "Studies for Terminal Area GNC of Reusable Launch Vehicles," AIAA Paper 2003-5438, Aug. 2003.

[23] Hull, J. R., Gandhi, N., and Schierman, J. D., "In-Flight TAEM/Final Approach Trajectory Generation for Reusable Launch Vehicles," AIAA Paper 2005-7114, Sept. 2005.

[24] Kluever, C. A., and Horneman, K. R., "Terminal Trajectory Planning and Optimization for an Unpowered Reusable Launch Vehicle," AIAA Paper 2005-6058, Aug. 2005.